



Biogenic Synthesis of Bismuth Oxide Nanoparticles and Its Antifungal Activity

KARUMALAIYAN PALANISAMY¹, VELAYUTHAM GURUNATHAN²
and JOTHILINGAM SIVAPRIYA^{3*}

¹Srinivasan College of Arts and Science (Affiliated to Bharathidasan University),
Perambalur District, Tamil Nadu-621212, South India.

²Department of chemistry, Bishop Heber College (Affiliated to Bharathidasan University),
Tiruchirappalli District, Tamil Nadu-620 017, South India.

³St. Joseph's Institute of Technology (Affiliated to Anna University), Chennai,
Tamil Nadu-600119, South India.

*Corresponding author E-mail: jothilingamsivapriyaj9390@gmail.com

<http://dx.doi.org/10.13005/ojc/390310>

(Received: April 11, 2023; Accepted: May 15, 2023)

ABSTRACT

The *Chenopodium album* extracts served as a capping agent in the present work to synthesize the Bi₂O₃ Nps. The synthesized nanoparticles were confirmed by various spectroscopic techniques. Nano-structured Bi₂O₃ was measured to have a mean size of 79.99nm. Anti-fungal activity of the synthesized Bi₂O₃ Nps was also evaluated. Bi₂O₃ Nps have been shown to have impressive antifungal efficacy against a variety of fungal species. It's a powerful anti-fungal medication that outperforms both plant extract and clotrimazole.

Keywords: Antifungal, Bismuth oxide, *Chenopodium album*, Green synthesis, XRD.

INTRODUCTION

Despite bismuth's proximity to other dangerous elements on the periodic table, the metal and its derivatives have been recognized to humans for thousands of years without causing any significant damage¹. Compared to sodium chloride, several bismuth substances have a lower toxicity². Because of this, bismuth is distinguished from other heavy metals and designated a "green element"¹. For instance, bismuth subsalicylate is prescribed for those experiencing diarrhoea in addition to

other symptoms (such as nausea, vomiting, and abdominal discomfort)³. Bismuth oxychloride gives beauty products and toiletries a metallic silver lustre. The product is sold as BIRON powder and has significant clinical uses.

The oxide of bismuth most often used in industry is bismuth trioxide (Bi₂O₃). It's used as a building block in the production of several chemical reagents and other bismuth-based products⁴. Bi₂O₃ has a unique polymorphism, with four different solid phases: monoclinic (α -Bi₂O₃), tetragonal



(β - Bi_2O_3), body-centered cubic (γ - Bi_2O_3), and triclinic (ω - Bi_2O_3)⁵. The α - Bi_2O_3 is generally stable at ambient temperatures and has a low solubility in water due to the presence of a surface hydroxyl group⁶. Since α - Bi_2O_3 is a basic oxide, the vast majority of its bonds are ionic in nature⁷. As it is utilized in dentistry substances to make these more transparent to X-rays than the underlying teeth surface⁸, it may find usage in biomedicine. AnuSol lotion, an astringent, an emollient, an antiseptic, and has Bi_2O_3 as one of its main ingredients⁹. As a homeostatic topical application, it may be considered to be utilized in free soft tissue transplants for oral injuries¹⁰. Further, it is tested as a possible drug for treating *Helicobacter pylori* diseases¹¹. Non-DNA locations are where bismuth substances are bio-coordinated, which opens up new possibilities for the development of novel mechanisms of action in chemotherapeutic agents¹².

While nanomaterials have a relatively high surface area, they are able to communicate with their biological targets more effectively. They can be used in the nanoformulations since they have different chemical and physical characteristics from the bulk versions. The fact that Bi_2O_3 nanoparticles are safe for human tissue¹³ means that they may be employed for a wide variety of applications, including those involving the measurement of temperature, the combination of imaging modalities, and the administration of therapeutic agents¹⁴. Anti-fungal, anti-bacterial, and anti-cancer properties of Bi_2O_3 nano-structures have been reported¹⁵⁻¹⁷. Multiple topologies are produced during the fabrication of Bi_2O_3 nanostructures using different chemical and physical approaches¹⁸.

Extracts from plants may play a role in the creation of metals and metal oxide nanostructures by acting as reducing and capping agents. Using non-toxic chemical ingredients and moderate reaction conditions is the technique to construct a greener method¹⁹. Because herbal phytochemicals facilitate the safest and also most cost-effective massive creation of biodegradable nanomaterials. Plants are able to produce a broad array of sophisticated nanostructures that equal the complexity of contemporary manufactured materials. Phytoconstituents that are water-soluble are accountable for the reduction²⁰. These include catechins, phenolic compounds, terpenoids, flavonoids, and alkaloids. The use of a green approach in the production of

nano-materials aids in reducing or removing the use of dangerous toxic pollutants. Efficient microbiological production of Bi_2O_3 nanoparticles through the phytopathogenic fungi *Fusarium oxysporum* has been reported by Uddin *et al.*,²¹. Employing tannic acid as a reductant, Aguirre *et al.*,²² produced β - Bi_2O_3 . Despite being produced via environmentally friendly methods, all of these technologies involve intricate methods and extended incubation periods. But Karnan *et al.*,²³ had designed and synthesized Bi_2O_3 nanoparticles via a green approach, although with a lengthy incubation and higher calcination temperature. Thus, it is important to create a straightforward, speedy, and completely environmentally friendly method for synthesising stabilized α - Bi_2O_3 nanoparticles. The production of α - Bi_2O_3 from chenopodium album leaf extract is reported for the first time in this work. For the production of α - Bi_2O_3 nanoparticles, aqueous extract of the leaf of *C. album* is used as a reductant and a stabilizing agents. The procedure is straightforward, quick, and really environmentally benign; moreover, it is very scalable.

MATERIALS AND METHOD

Chemicals

Nice and Loba chemicals were used for all of the material acquisition. The reactions took place in very pure solvents that required no additional processing.

Plant material collection

Chenopodium album was gathered from the marketplaces around the Trichirappalli region. The fresh leaves of plant was employed for the production of bismuth oxide Nps.

Plant extract preparation

Fresh leaves of the *Chenopodium album* plant were used to produce the extract solution. Leaves of a newly harvested plant that have been thoroughly washed in de-ionized water and then chopped very finely. Finally, after boiling the plant leaves in 100 mL of distilled water at 100°C, the resulting liquid was filtered and stored at 4°C for advance usage in the experiments.

Synthesis of Bismuth oxide nanoparticles

Bismuth oxide nanoparticles were made by dissolving 0.1g of $\text{Bi}(\text{NO}_3)_3 \cdot 5\text{H}_2\text{O}$ in a sufficient

volume of de ionised water and then combining that solution with 10 mL of a leaf extract, while stirring at room temperature through a magnetic stirrer at 1000 rpm for 3 hours. The pH of the reaction medium was attuned via adding 1 mL of 10% NaOH solution. The solid that had been precipitated was drained and dried. It took 12 h in the oven at 150°C to refine the raw material. After three hours of calcination at 500°C, the resulting material was ground into a fine powder utilising mortar and pestle.

Antifungal activity

The *In-vitro* antifungal activity of the synthesized Bi_2O_3 Nps and plant extract were evaluated by disc diffusion method. 100 μL of extract and the synthesized Bismuth oxide NPs were tested against 4 fungal pathogens. All the test samples were loaded in the pre-prepared petri plates which is having the respective medium. After 32 h, the zone of the each sample measured by millimeter scale²⁴.

RESULTS AND DISCUSSION

UV-Visible

Bismuth oxide NPs are formed when a UV-visible absorption peak appears between 200 and 400nm. The specific SPR band for smaller Bismuth oxide NPs is guided by the significant absorption peak seen at 234nm in our study. The UV-Vis spectra of fabricated Bi_2O_3 NPs are displayed in Figure 1.

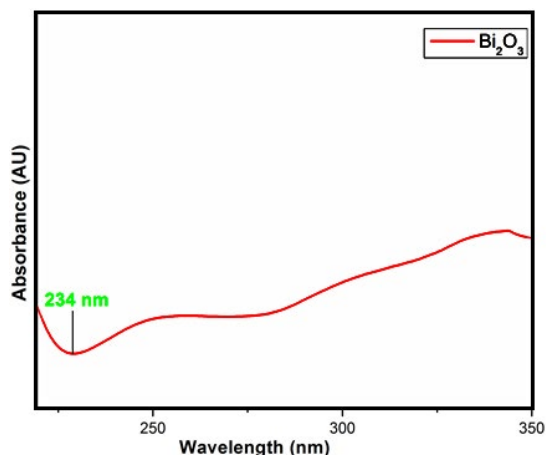


Fig. 1. UV-Vis spectrum of Bi_2O_3 Nps

FT-IR

FT-IR spectra measured between 400 and 4000 cm^{-1} . A broad band at 3400.00 cm^{-1} is consistent with the NH moiety that could be present due to the presence of alcohol. Alkanes belonging

to the C-H functional group are shown by the peaks at 2800-3000 cm^{-1} . The carbonyl moiety contributed the C-O and C=O bands at 1601 and 1396 cm^{-1} . Because of the presence of Bi-O-Bi linkage, a characteristic peak can be seen at 829 cm^{-1} . Band of intense absorption at 442 cm^{-1} results from Bi-O mode. It squares with the information provided in the cited work. Bismuth oxide is responsible for the observable significant peaks at 442, 470, and 510 cm^{-1} . FT-IR testing verified that Bi_2O_3 NPs formed and also found evidence of functional groups in the capping agent. Bi_2O_3 NPs were produced, and their FT-IR spectra are shown in Figure 2.

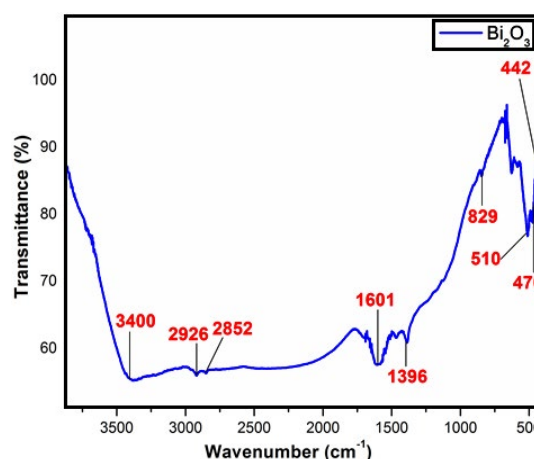


Fig. 2. FT-IR spectrum of Bi_2O_3 Nps

SEM and Mapping

SEM (scanning electron microscopy), was used in order to control the size and shape of the produced bismuth oxide nanoparticles (NPs). The spherical form of the generated Bismuth oxide NPs was verified by SEM as displayed in Fig. 3. Bismuth oxide NPs were uniform in size and shape after synthesis. Researchers used SEM mapping to confirm that the produced nanoparticle was really Bismuth oxide. Each red dot symbolizes a single atom of bismuth, and each green dot an individual atom of oxygen. SEM mapping experiments performed on Bismuth oxide Nps are shown in Figure 4.

EDX

EDX examination verified the elemental makeup of the produced Bi_2O_3 NPs. Bismuth oxide nanoparticles (NPs) were proven to be the produced material due to the appearance of zinc and oxygen atoms in the EDX spectra (Fig. 5). Specifically, 7.42% of the atomic weight was attributed to bismuth, and 92.58% to oxygen. The presence of bioorganics or contaminants in the solutions could account for the

occurrence of additional peaks in the spectrum. Table 1 shows the elemental make-up of a nanoparticle of bismuth oxide.

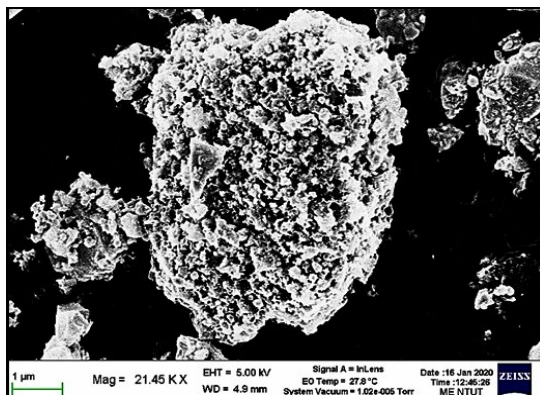


Fig. 3. SEM image of Bi_2O_3 Nps

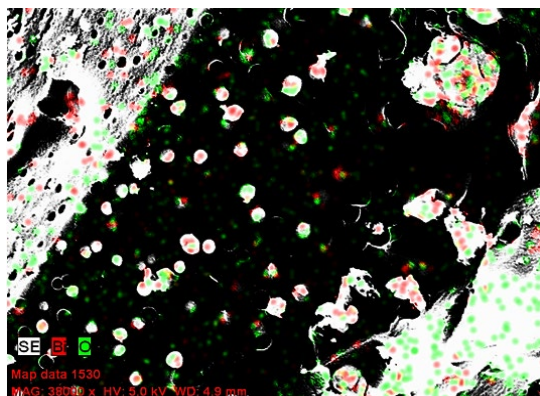


Fig. 4. SEM mapping of Bi_2O_3 Nps

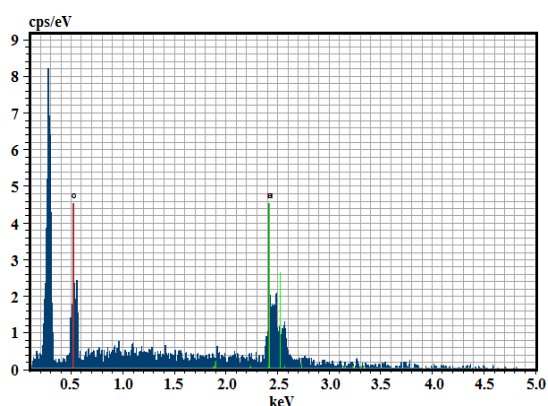


Fig. 5. EDX spectra of Bi_2O_3 Nps

Table 1: Elemental conformation of Bi_2O_3 Nps

Element	Atomic number	Atom%	Weight%	Weight % Error
O	8	51.14	7.42	1.70
Bi	83	48.86	92.58	5.10
Total	-	100.00	100.00	-

XRD Analysis

Bismuth oxide NPs were produced, and their XRD pattern is shown in Fig. 6. Pure monoclinic structure of Bismuth oxide NPs was identified by diffraction peaks at $2\theta = 25.2^\circ, 26.4^\circ, 27.4^\circ, 27.8^\circ, 28.2^\circ, 33.6^\circ, 34.8^\circ, 37.6^\circ, 46.2^\circ, 48.3^\circ, 54.8^\circ$ and 67.3° , which were indexed to (102), (002), (-111), (120), (012), (211), (200), (-112), (223), (311), (241) and (341) planes. Bismuth oxide NPs, as expected, were found to have diffraction peaks that were consistent with those observed. All of the diffraction peaks correspond rather well with the typical arrangement for pure Bismuth oxide nanoparticles (JCPDS No. 01-076-1730). These prominent peaks are indicative of the highly crystalline character of the produced nanoparticles. The average crystallographic size may be determined from the observed primary diffracted peak by using the Scherer equation,

$$D_{(hkl)} = \frac{k\lambda}{\beta \cos\theta}$$

The average crystallite size of the produced Bi_2O_3 Nps was 79.99nm.

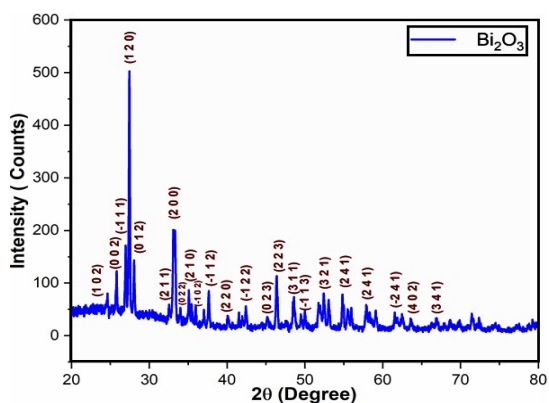


Fig. 6. XRD spectra of Bi_2O_3 Nps

Antifungal activity

The antifungal efficacy of the manufactured Bi_2O_3 Nps and fresh leaf extract against four distinct fungus species was evaluated. Compared to *Chenopodium album*, the Bi_2O_3 Nps exhibits exceptional antifungal effectiveness. In tests with *C. albicans* and *M. audouinii*, two fungal species, Bi_2O_3 Nps exhibits strong antifungal activity. As compared to control clotrimazole, which had a MIC value of 02 $\mu\text{g}/\text{mL}$, Bi_2O_3 Nps was much more active. In *M. audouinii*, Bi_2O_3 Nps with a MIC value of 02 $\mu\text{g}/\text{mL}$ exhibits significant antifungal effect than clotrimazole with a MIC value of 04 $\mu\text{g}/\text{mL}$. Table 2 provided a summary of the findings.

Table 2: Antifungal activity of chenopodium album leaf extract and Bi₂O₃ Nps

Compds	MIC (µg/mL)*			
	<i>Aspergillus niger</i>	<i>Candida albicans</i>	<i>Microsporium audouinii</i>	<i>Cryptococcus neoformans</i>
Plant extract	52	18	32	24
Bi ₂ O ₃	46	01	02	18
Clotrimazole	01	02	04	05

#Values are the means of ±SD

CONCLUSION

In conclusion, *Chenopodium album* leaf extract was used for the first time to effectively produce Bi₂O₃ Nps in under 3 h utilizing a straightforward, eco-friendly, and green technique. This methodology eliminates the drawbacks of the traditional procedures mentioned in the prior literature²⁵⁻²⁸, such as lengthy incubation periods, extremely high temperature and pressure settings, complicated and costly apparatus, and time-consuming reactions. As a potential reducing and capping agent in nanoparticle production, *Chenopodium album* leaf extract helps keep the synthesis process gentle. The synthesized Nps were assessed for antifungal activity towards various pathogenic fungi. Compared to *Chenopodium album*

leaf extract and clotrimazole, Bi₂O₃ Nps are a more effective fungicide.

ACKNOWLEDGMENT

All the Authors thank the management of Srinivasan College of Arts and Science, Perambalur District, Tamil Nadu, South India, Bishop Heber College, Tiruchirappalli District, Tamil Nadu, South India and St. Joseph's Institute of Technology (Affiliated to Anna University), Chennai, Tamil Nadu, South India for their constant support and providing the lab facility to do the research work.

Conflict of Interests

There is no conflict of interest

REFERENCES

- Mohan, R., *Nat. Chem.*, **2010**, *2*, 336-336.
- Suzuki, H.; Komatsu, N.; Ogawa, T.; Murafuji, T.; Ikegami, T.; Matano, Y. *Organobismuth chemistry*. Elsevier., **2001**.
- Figuroa-Quintanilla, D.; Salazar-Lindo, E.; Sack, R. B.; Leon-Barua, R.; Sarabia-Arce, S.; Campos-Sanchez, M.; Eyzaguirre-Maccan, E. *N. Engl. J. Med.*, **1993**, *328*, 1653-1658.
- Kelly, Z.; Ojebuoboh, F. *JOM.*, **2002**, *54*, 42-45.
- Mehring, M. *Coord. Chem. Rev.*, **2007**, *251*, 974-1006.
- Cox, P.A. 'The elements: their origin, abundance, and distribution' (Oxford University Press, Oxford., **1989**)
- Earnshaw, A.; Greenwood, N. N. 'Chemistry of the elements' (Pergmon Press Ltd, Oxford, **1984**, 1st edn.)
- Josette, C. *J. Endod.*, **2014**, *40*, 436-440.
- 'AnuSol Cream'. Available at <https://www.medicines.org.uk/emc/medicine/7159>, accessed February **2023**.
- Kim, S. H.; Tramontina, V. A.; Papalexiou, V.; Luczyszyn, S. M. *Quintessence Int.*, **2010**, *41*, 645-649.
- Ketata, M.; Desjardins, Y.; Ratti, C. *J. Food Eng.*, **2013**, *116*, 202-212.
- Tiekink, E. *Crit. Rev. Oncol. Hematol.*, **2002**, *42*, 217-224.
- 'Bismuth trioxide toxicology'. Available at http://digitalfire.com/4sight/hazards/ceramic_hazard_bismuth_trioxide_toxicology_252.html, accessed February., **2023**.
- Zhu, H.; Li, Y.; Qiu, R.; Shi, L.; Wu, W.; Zhou, S. *Biomaterials.*, **2012**, *33*, 3058-3069.
- Hernandez-Delgadillo, R.; Velasco-Arias, D.; Martinez-Sanmiguel, J. J.; Diaz, D.; Zumeta-Dube, I.; Arevalo-Niño, K.; Cabral-Romero, C. *Int. J. Nanomedicine.*, **2013**, *8*, 1645-1652.
- Aggrawal, S.; Chauhan, I.; Mohanty, P. *Mater. Express.*, **2015**, *5*, 429-436.
- Anusha, S.; Anandakumar, B. S.; Mohan, C. D.; Nagabhushana, G. P.; Priya, B. S.; Rangappa, K. S. *RSC Adv.*, **2014**, *4*, 52181-52188.

18. Huang, Q.; Zhang, S.; Cai, C.; Zhou, B. *Mater. Lett.*, **2011**, *65*, 988-990.
19. Korbekandi, H.; Iravani, S. 'Biological synthesis of nanoparticles using algae', in Rai, M., Posten, C., (Eds.): 'Green biosynthesis of nanoparticles: mechanisms and applications' CABI, Wallingford, UK., **2013**, 53-60.
20. Mohammadinejad, R.; Karimi, S.; Iravani, S.; Varma, R. S. *Green Chem.*, **2016**, *18*, 20-52.
21. Uddin, I.; Adhyntaya, S.; Syed, A. *J. Nanosci. Nanotechnol.*, **2008**, *8*, 1-5.
22. Aguirre, F. M. A.; Becerra, R. H. *Appl. Phys. A.*, **2015**, *119*, 909-915.
23. Karnan, T.; Selvakumar, S. A. S.; Adinaveen, T.; Suresh, *J. Int. J. Sci. Eng. Res.*, **2016**, *7*, 266-270.
24. Indurkar, A. R.; Sangoi, V. D.; Patil, P. B.; Nimbalkar, M. S. *IET nanobiotechnology*. **2018**, *12*, 496-499.
25. Oudghiri-Hassani, H.; Rakass, S.; Wadaani, F. T. A.; *J. Taibah Univ. Sci.*, **2015**, *9*, 508-512.
26. Madler, L.; Pratsinis, S. E. *J. Am. Ceram. Soc.*, **2002**, *85*, 1713-1718.
27. Huang, X.; Zhang, W.; Tan, Y. *Ceram. Int.*, **2016**, *42*, 2099-2105.
28. Dayana Jeyaleela, G.; Irudaya Monishaa, A.S; Rosaline Vimala, J; Anitha Immaculate, A. *Int. J. Pharm. Pharm. Sci.*, **2017**, *9*(10), 67-72.